Supporting Information

Das et al. 10.1073/pnas.1409667112

In cells, the Rac1 FRET sensor molecules can be either in the GTP-bound state or the GDP-bound state. Our goal is to estimate the fraction of the GTP-bound molecules, η from the FRET imaging data. In ratiometric FRET imaging, one typically computes the ratio between the FRET channel signal intensity and the donor channel intensity,

$$R = \frac{\eta FT + (1-\eta)FD}{\eta DT + (1-\eta)DD} \quad \textbf{[S1]}$$

where the symbol F and D represent the fluorescent intensities of the FRET and donor channels, respectively; and the subscript T and D denotes the GTP- and GDP-bound subpopulation.

By defining three new constants, $R_T = F_T/D_T$, $R_D = F_D/D_D$, and $\beta = D_D/D_T$, we can easily rearrange Eq. **S1** as

$$R = \frac{\eta RT + (1-\eta)\beta\, RD}{\eta + (1-\eta)\beta} \quad \textbf{[S2]}$$

and therefore,

$$\eta = \left[1 + \frac{(R_T - R)}{\beta(R - R_D)}\right]^{-1}. \quad \textbf{[S3]}$$

Now consider a cell with polarized Rac1 signaling. We can typically define an active region, where the FRET ratio, R_2, is higher than an inactive region, which has an average FRET ratio of R_1. To quantitatively compare the η values at these two spatial regions, we define a polarization factor χ_{ex} as the ratio of η values: $\chi_{ex} = \frac{\eta 2}{\eta 1}$. By applying Eq. **3**, we can reach that

$$\chi_{ex} - 1 = \left[\frac{\beta - 1}{R_T - R_D} + 1\right]^{-1} \frac{R_2 - R_1}{(R_1 - R_D)(R_2 - R_D)}. \quad \textbf{[S4]}$$

It is important to note that R_T, R_D, and β are all calibration constants that can be obtained from measurements of control constructs.

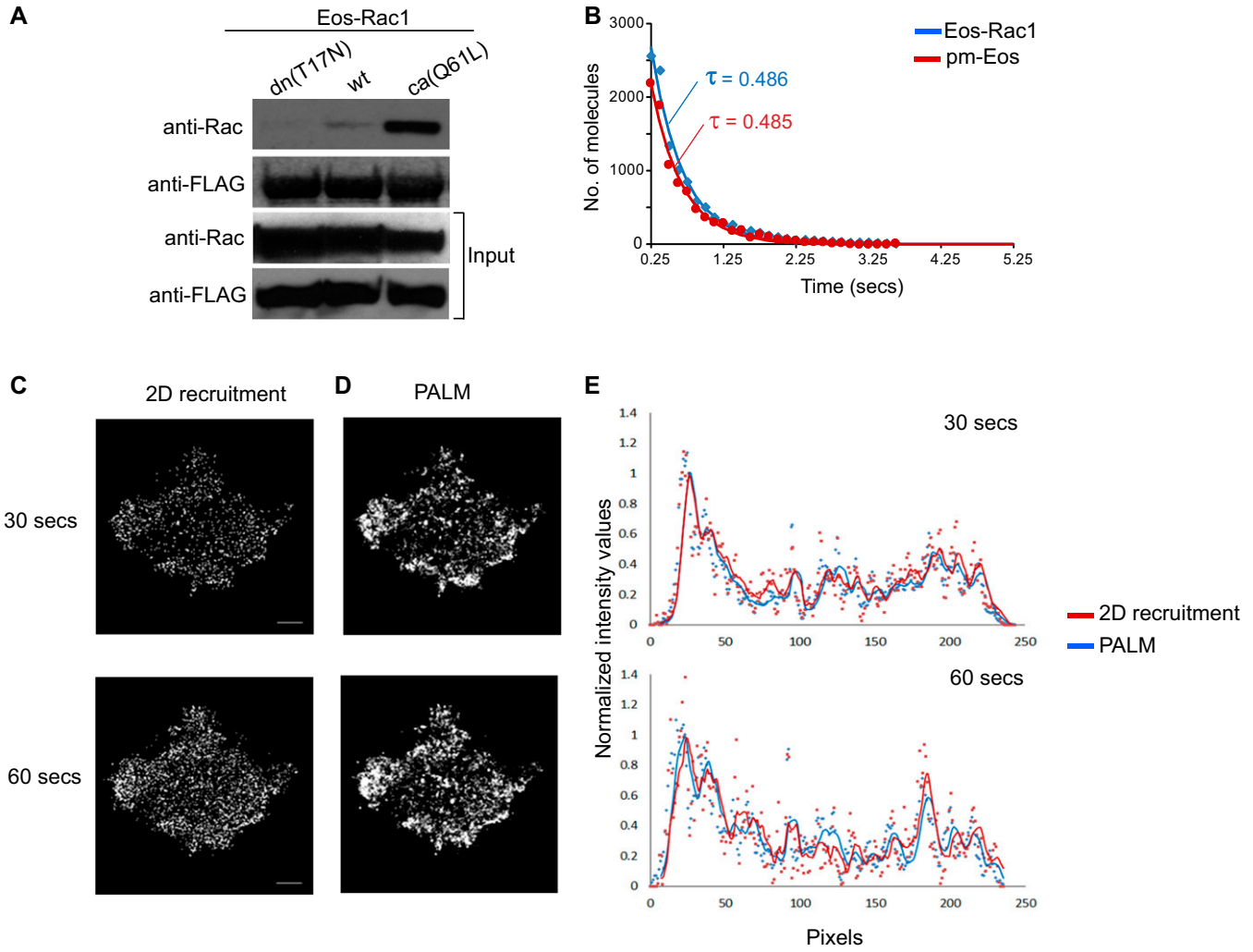

Fig. S1. Characterization of Eos-Rac1 and SPT measurements. (*A*) Pulldown of Eos-Rac1 constructs with FLAG-PAK as the bait, and blotting for Rac and FLAG, showed strongest interaction for caRac1. The input blots for Rac and FLAG-PAK shown for all of the constructs. (*B*) Trajectory duration histograms of Eos-Rac1 (blue) and pm-Eos construct (red) as a function of time. The solid lines represent fitting with a single exponential decay function to yield time constant τ. (*C* and *D*) Single-molecule imaging performed on MCF-7 cells expressing Eos-wtRac1 after plating on collagen-coated dishes. The 2D recruitment maps (*C*) indicate the first point (initial position) of all single-molecule trajectories of Rac1 on the plasma membrane. PALM maps (*D*) were plotted indicating all of the positions of molecules along individual trajectories. (*E*) Intensity profile of 2D recruitment and PALM maps were matched pixel by pixel for 30 s and 60 s of image acquisition. Both maps show similar profiles, indicating that the binding event (recruitment) is a true representation of the localization of the single-molecule trajectories. Scale bar corresponds to 5 μm.

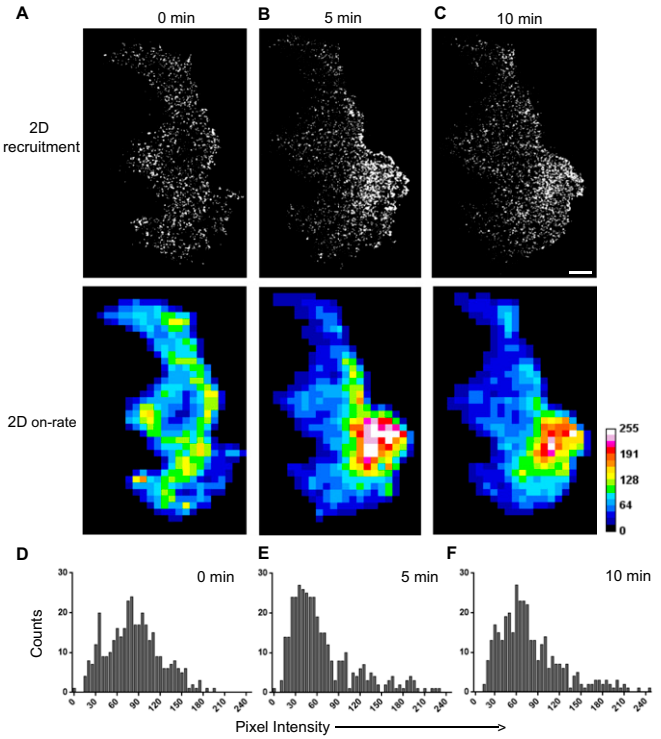

Fig. S2. Spatial polarization of Rac1 recruitment to lamellipodia. (*A*–*C*) MCF-7 cells expressing Eos-wtRac1 spreading on collagen show expansion of lamellipodia. The 2D recruitment and 2D on-rate maps for different time points of imaging show increased membrane Rac1 recruitment to lamellipodia. (*D*–*F*) Representative gray value histograms of 2D on-rate maps for all time points are shown. Scale bar corresponds to 5 μm.

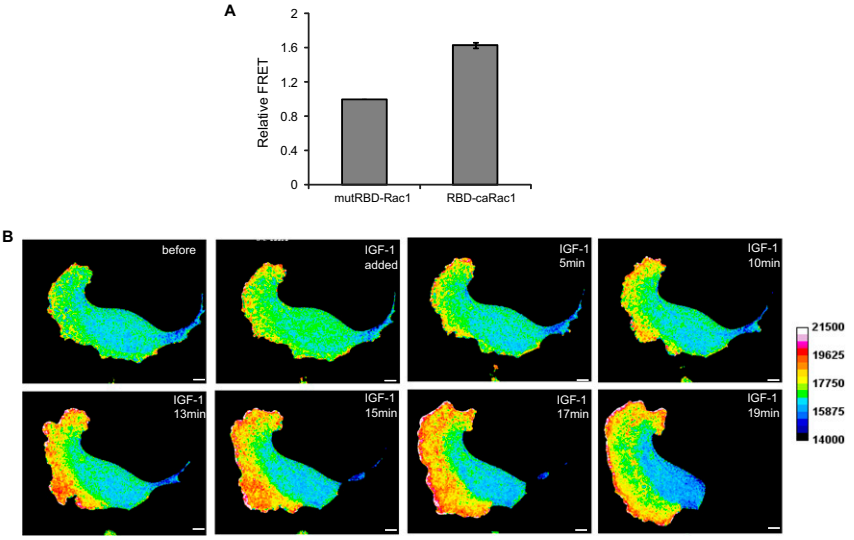

Fig. S3. Measurement of FRET efficiency of Rac1 FRET sensor. MCF-7 cells expressing "mutant" (mutRBD-Rac1) and "constitutively active" (RBD-caRac1) sensor were analyzed with conventional wide-field FRET imaging by excitation with 440-nm light. (*A*) The graph shows the FRET ratio normalized to that of the mutant sensor. Error bars represent SEM from 17 cells measured for both constructs. (*B*) Ratiometric (FRET/Cer3) wide-field fluorescence images of cells expressing Rac1 FRET sensor after induction with growth factor IGF1 (50 ng/mL). Expansion of lamellipodia associated with increased FRET activity (warmer colors). Scale bar corresponds to 5 μm.

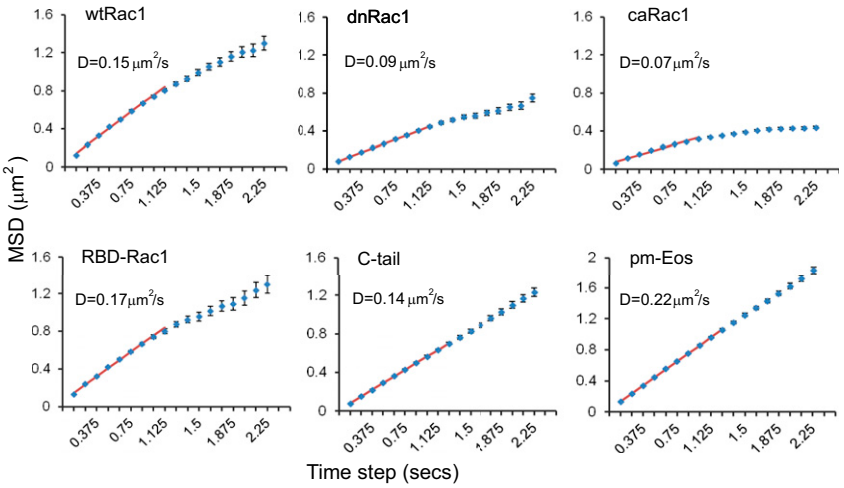

Fig. S4. Effective ensemble diffusion of different Rac1 constructs. Ensemble averaged MSD traces generated from single-molecule trajectories of wt and mutant Rac1 and pm-Eos molecules. The effective diffusion coefficient (D) is computed from the slope (straight line fitting) of the first to ninth time step (ΔT = 125 ms).

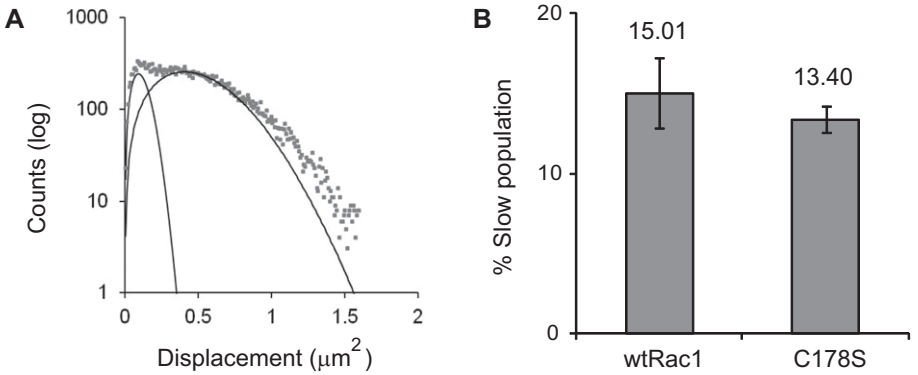

Fig. S5. Effect of palmitoylation of Rac1 on membrane diffusion. MCF-7 cells expressing Eos-labeled C178S-Rac1 construct were imaged. (*A*) Histograms of 2D displacement (ΔT = 125 ms) of the molecules fitted with a bicomponent 2D diffusion model exhibited both slow (0.0419 ± 0.002 μm²/s) and fast diffusing populations (1.075 ± 0.099 μm²/s). (*B*) The graph demonstrates the percentage of molecules belonging to the slow diffusing (D_1) population is comparable between wtRac1 and C178S-Rac1. Error bars represent SEM for cells. Values represent data pooled from several independent experiments wtRac1 (10 cells, 5.9×10^4 trajectories) and C178S (8 cells, 4.6×10^4 trajectories).

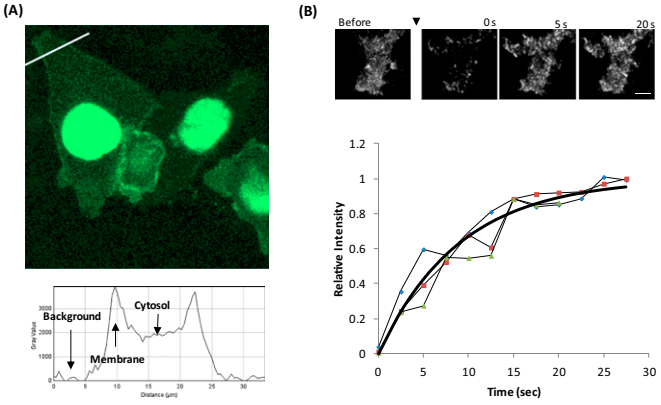

Fig. S6. C-tail dynamic turnover at cell membrane. (*A*) Confocal image and line scan of MCF7 cells expressing Rac1 C-Tail. Image acquired at 0.7-μm axial resolution. (*B*) TIR-FRAP analysis of RFP-Rac1-C-Tail. After selectively photobleaching signal at plasma membrane by a strong TIRF illumination, the fluorescence recovery was monitored with time-lapse images with 2.5-s intervals (results from three cells are shown). Black line is the best exponential fit.

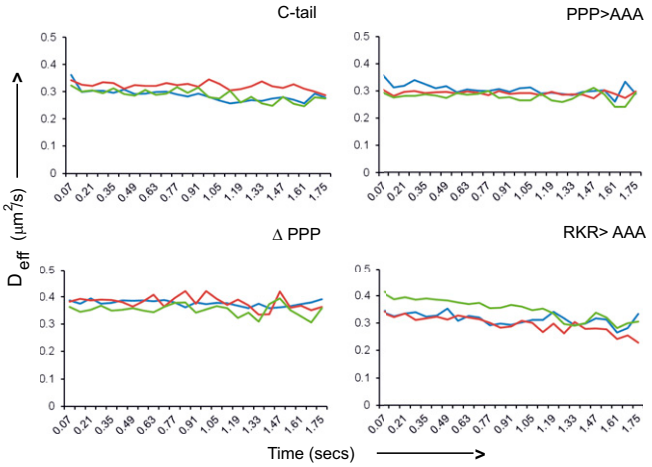

Fig. S7. Effective mobility of Rac1 C-terminal tail. The average effective diffusion coefficients were plotted as a function of time (ΔT = 70 ms) to determine the changes in mobility upon membrane binding. Each color represents a different cell. There is no apparent decay in mobility for all C-terminal tail constructs, and thus no fitting was done.

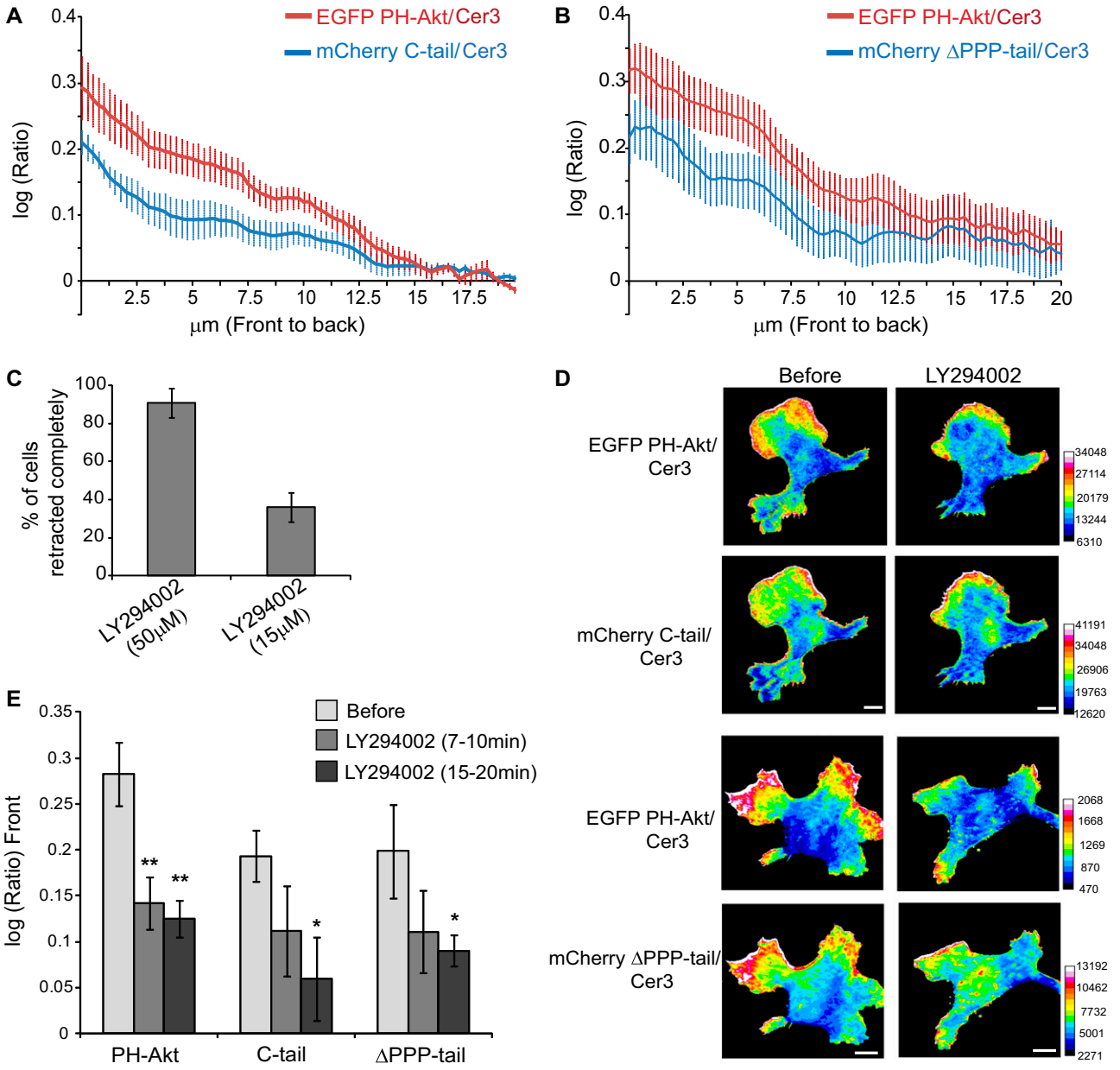

Fig. S8. PI3K gradient and activity is critical for Rac1 recruitment at the protrusions. MCF-7 cells coexpressing EGFP-PH(Akt), mCherry-Rac tail, and Cer3 constructs were imaged by TIRF illumination under cell spreading conditions. Ratiometric images were obtained for both EGFP-PH (Akt)/ Cer3 and for mCherry-Rac tail/ Cer3 (C-tail and ΔPPP tail). (*A* and *B*) Intensity measurements of the ratiometric images using a 5-μm-band scan from the front to the back of the protrusions reveal a gradient for both PH(Akt) and Rac tail (C-tail and ΔPPP tail). Time-averaged measurements of protrusions from 10 different cells are shown. (*C*) Quantification of cellular morphology change after PI3K inhibition using two doses of LY294002 (50 μM and 15 μM) during cell spreading from 25 cells. (*D*) Ratiometric images corresponding to EGFP-PH (Akt)/ Cer3 and mCherry-Rac tail/ Cer3 for the same cells before and after PI3K inhibition (15 μM LY294002). Retraction of the protrusion evident after 15 min of LY294002 treatment. Warmer colors indicate increased concentration of molecules. (*E*) Quantification of the intensity at the front of the protrusion (1.5 μm from leading edge) before and after LY294002 treatment. Values for "Before" were obtained by averaging each protrusion over 10 min. Data from three cells for mCherry-C-tail and for mCherry-ΔPPP-tail, and six cells for EGFP-PH(Akt). Error bars represent SEM. *$P < 0.05$ wrt "Before" treatment. Scale bar is 10 μm.

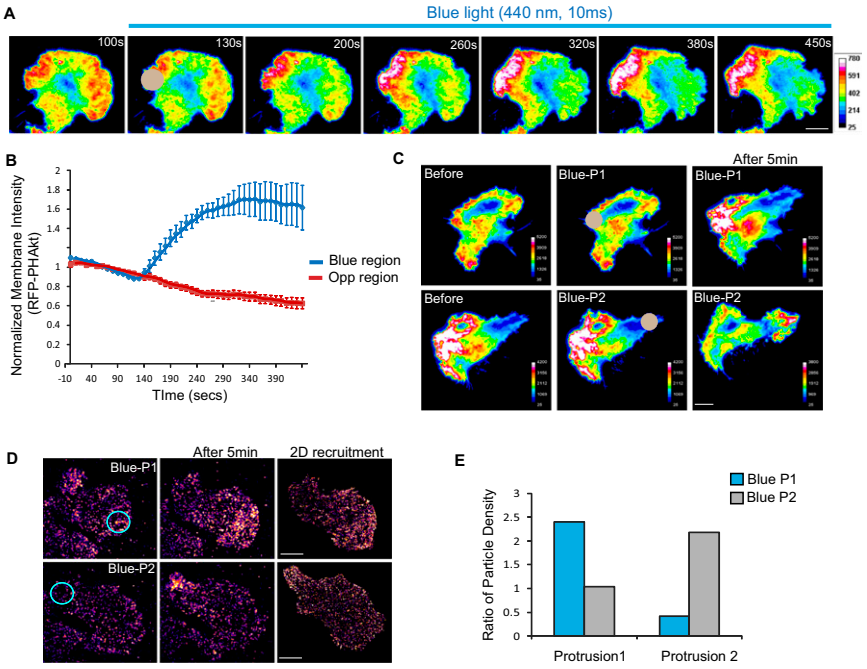

Fig. S9. Blue-light-induced PI(3,4)P_3 synthesis and polarization in cells. MCF-7 cells coexpressing the CIBN-CAAX, Cry2-iSH, and RFP-PH(Akt) constructs were imaged under TIRF illumination. (*A*) TIRF Images of RFP-PH(Akt) before and after blue-light illumination (440 nm, 10 ms) indicate the intensity fluctuations [warmer colors represent higher membrane-bound PH(Akt)]. The gray circle shows the illumination spot. (*B*) Representative graphs indicate the normalized intensity of membrane PH(Akt) in illumination region (blue line) versus a region opposite to illumination spot (red line). (*C*) Micrographs of a cell subjected to sequential illumination in two opposite regions (indicated by filled gray circles), Blue-P1 and Blue-P2. First and second panels show the snapshots before, during, and after 5 min of local illumination for Blue P1 and Blue P2, respectively. (*D*) TIRF Eos images of a cell expressing CIBN-CAAX, Cry2-iSH, and Eos-Rac1 (C-tail), subjected to sequential blue-light illuminations, Blue-P1, and Blue-P2. After 5 min of blue-light illumination, single-molecule imaging of Rac1 C-tail was performed to generate 2D recruitment maps. (*E*) Ratio of Rac1 particle density from protruding versus nonprotruding region was calculated for Protrusion 1 (formed during Blue P1) and Protrusion 2 (formed during Blue P2) for sequential illumination regimes. Scale bar corresponds to 10 μm. Error bars for PH(Akt) represent SEM from nine cells from three independent experiments.

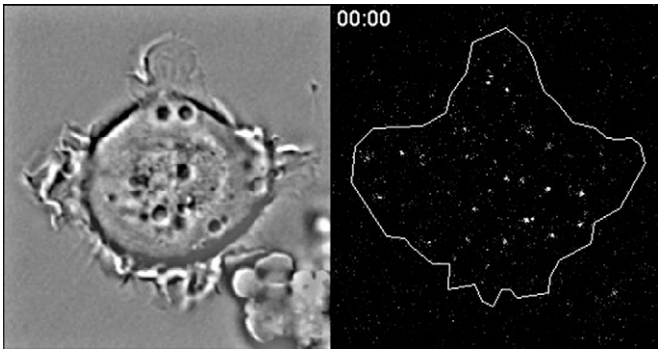

Movie S1. Single-molecule imaging of membrane-associated Rac1 molecules in MCF-7 cells expressing Eos-wtRac1, after being plated on to collagen-coated dishes. Time interval is 125 ms.

Movie S1

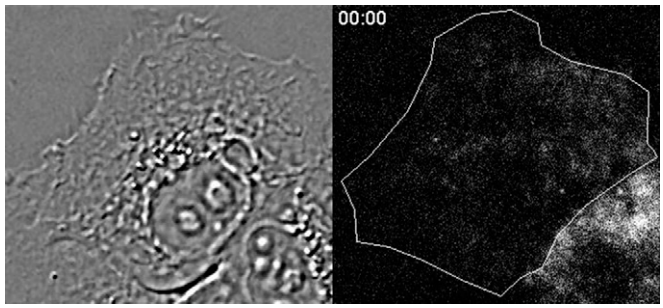

Movie S2. Single-molecule imaging of Rho-GDI molecules in MCF-7 cells expressing Eos-RhoGDI, after being plated on to glass-bottom dishes. Time interval is 125 ms.

Movie S2

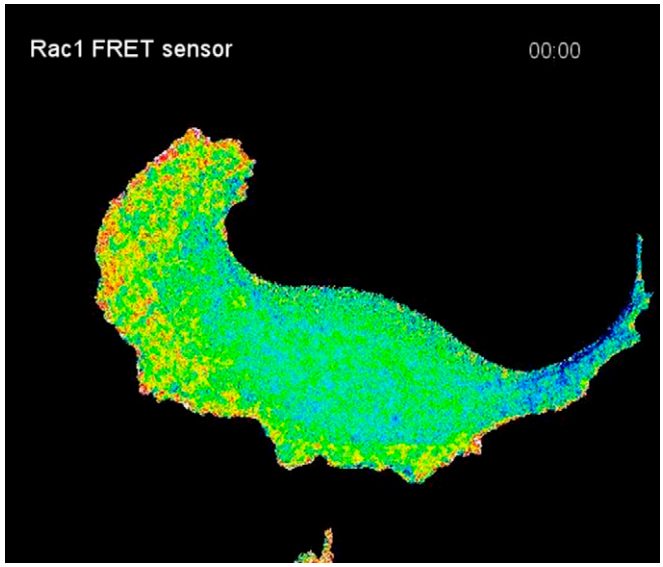

Movie S3. Ratiometric (FRET/Cer) imaging of a MCF-7 cell expressing Rac1-FRET sensor. The cells were imaged 1 h after plating on collagen-coated dishes and IGF1 (50 ng/mL) was added at fifth frame (4 min 40 s). Time interval is 1 min 10 s. Warmer colors indicate higher Rac1 activity.

Movie S3

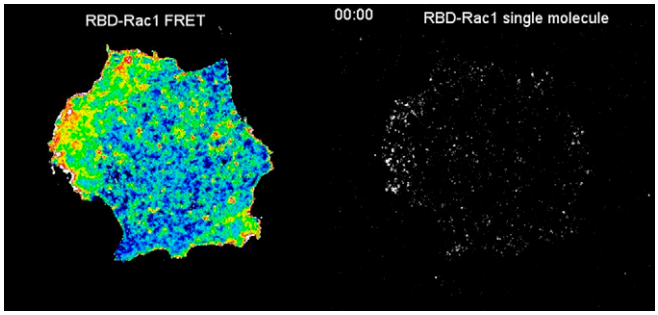

Movie S4. Single-molecule imaging of Rac1 sensor (RBD-Rac1) in MCF-7 cells plated on to collagen-coated dishes. The higher membrane recruitment corresponds to higher FRET activity in the left panel. Time interval is 150 ms.

Movie S4

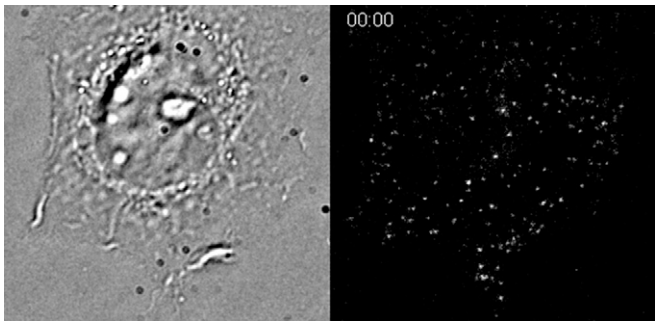

Movie S5. Single-molecule imaging of Rac1 C-tail in MCF-7 cells, after being plated on to collagen-coated dishes. Time interval is 70 ms.

Movie S5

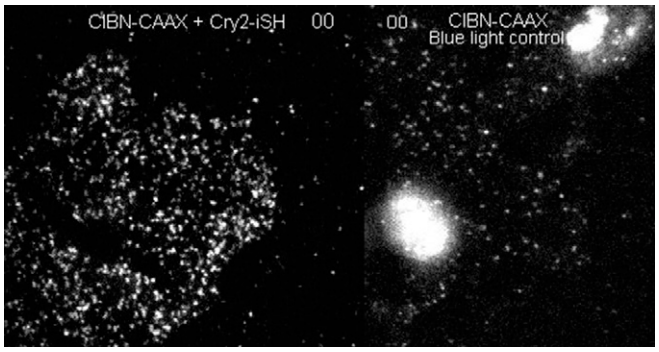

Movie S6. Single-molecule imaging of membrane Rac1 (C-tail) in MCF-7 cells coexpressing CIBN-CAAX, Cry2-iSH (left panel), or coexpressing CIBN-CAAX (right panel), during local blue-light illumination (440 nm, 10 ms). The blue circle indicates the illumination spot. Time interval is 10 s.

Movie S6

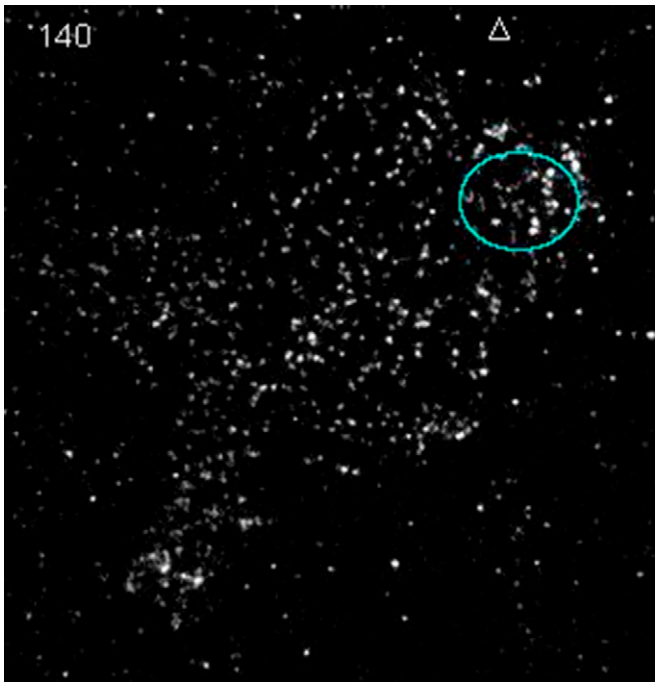

Movie S7. Single-molecule imaging of membrane Rac1 (ΔPPP tail) in MCF-7 cells coexpressing CIBN-CAAX, Cry2-iSH, and Eos-ΔPPP tail, during local blue-light illumination (440 nm, 10 ms). The blue circle indicates the illumination spot. Time interval is 10 s.

Movie S7

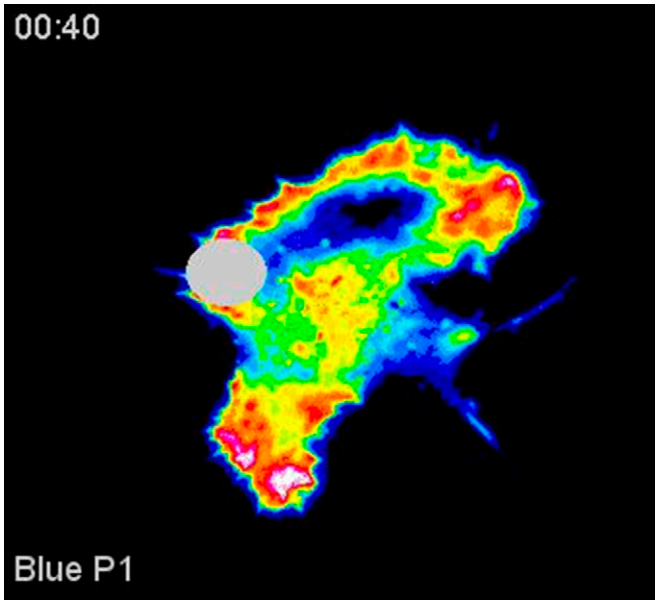

Movie S8. Imaging of $PI(3,4)P_3$ probe RFP-PH(Akt) under TIRF illumination in MCF-7 cells coexpressing CIBN-CAAX, Cry2-iSH, and RFP-PH(Akt). Higher intensity of the membrane-bound probe corresponds to warmer colors. Change in polarization of cells is indicated by sequential blue-light illumination (440 nm, 10 ms) in two regions: Blue P1 and Blue P2. Solid gray circle indicates the beginning of blue-light illumination, shown in the subsequent frames by open gray circles. Time interval is 10 s.

Movie S8

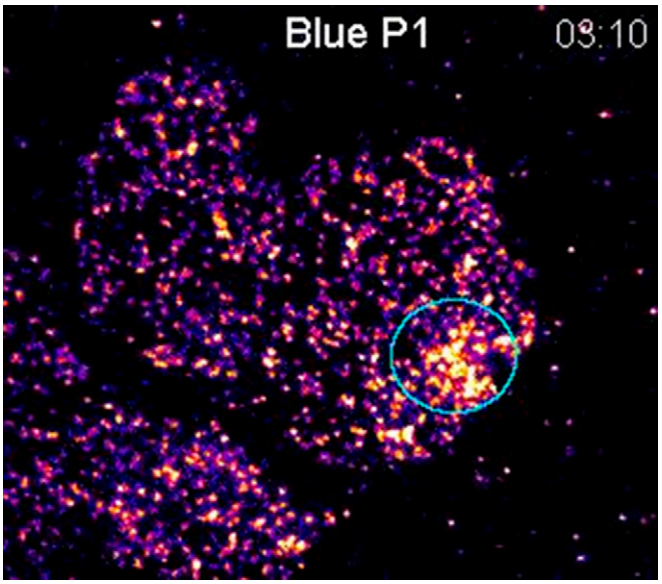

Movie S9. Imaging of membrane-bound Rac1 (C-tail) molecules in MCF-7 cells coexpressing CIBN-CAAX, Cry2-iSH, and Eos-C-tail. Warmer colors indicate higher density of Rac1 molecules. Sequential blue-light illumination (440 nm, 10 ms) was done in two regions: Blue P1 and Blue P2. Solid gray circle indicates the beginning of blue-light illumination, shown in the subsequent frames by open gray circles. Time interval is 10 s.

Movie S9